Available online at www.sciencedirect.com

SCIENCE DIRECT

Biochimica et Biophysica Acta 1715 (2005) 6 – 18

BIOCHIMICA ET BIOPHYSICA ACTA
BBA

http://www.elsevier.com/locate/bba

Membrane association and activity of 15/16-membered peptide antibiotics: Zervamicin IIB, ampullosporin A and antiamoebin I

T.N. Kropacheva[a], E.S. Salnikov[b], H.-H. Nguyen[c], S. Reissmann[c], Z.A. Yakimenko[d], A.A. Tagaev[d], T.V. Ovchinnikova[d], J. Raap[e,*]

[a]*Chemistry Department, Udmurt State University, Izhevsk, Russia*
[b]*Institute of Chemical Kinetics and Combustion, Academy of Sciences, Novosibirsk, Russia*
[c]*Institute of Biochemistry and Biophysics, Friedrich-Schiller-University, Jena, Germany*
[d]*Shemyakin-Ovchinnikov Institute of Bioorganic Chemistry, Moscow, Russia*
[e]*Leiden Institute of Chemistry, Gorlaeus Laboratories, University of Leiden, P.O. Box 9502, 2300RA, Leiden, The Netherlands*

Received 24 December 2004; received in revised form 14 June 2005; accepted 7 July 2005
Available online 8 August 2005

Abstract

Permeabilization of the phospholipid membrane, induced by the antibiotic peptides zervamicin IIB (ZER), ampullosporin A (AMP) and antiamoebin I (ANT) was investigated in a vesicular model system. Membrane-perturbing properties of these 15/16 residue peptides were examined by measuring the K^+ transport across phosphatidyl choline (PC) membrane and by dissipation of the transmembrane potential. The membrane activities are found to decrease in the order ZER > AMP >> ANT, which correlates with the sequence of their binding affinities. To follow the insertion of the N-terminal Trp residue of ZER and AMP, the environmental sensitivity of its fluorescence was explored as well as the fluorescence quenching by water-soluble (iodide) and membrane-bound (5- and 16-doxyl stearic acids) quenchers. In contrast to AMP, the binding affinity of ZER as well as the depth of its Trp penetration is strongly influenced by the thickness of the membrane ($diC_{16:1}$PC, $diC_{18:1}$PC, $C_{16:0}/C_{18:1}$PC, $diC_{20:1}$PC). In thin membranes, ZER shows a higher tendency to transmembrane alignment. In thick membranes, the in-plane surface association of these peptaibols results in a deeper insertion of the Trp residue of AMP which is in agreement with model calculations on the localization of both peptide molecules at the hydrophilic–hydrophobic interface. The observed differences between the membrane affinities/activities of the studied peptaibols are discussed in relation to their hydrophobic and amphipathic properties.

Keywords: Peptaibol; Bilayer; Conductance; Channel formation; Transmembrane; Amphipathicity

1. Introduction

Peptaibols are linear peptides, highly enriched with helix-promoting α-aminoisobutyric acid (Aib) or isovaline (Iva) residues, acylated at the N-terminus and bearing an amino alcohol at the C-terminus. Peptaibols, ranging in length from 5 to 20 residues, are isolated from fungal sources and presently include more than 300 members (alamethicins, suzukacilins, zervamicins, antiamoebins, ampullosporins, trichogins, etc). They show a wide spectrum of biological activities which are thought to be correlated with their ability to permeate cell membranes, in particularly by making transmembrane pores (channels) [1]. Most of the studies are concentrated on the 20-residue long alamethicin (ALA), which is capable to form voltage-gated channels with a number of features common with some native channel proteins [2, 3]. Characterization of the shorter chain peptaibols received relatively less attention and the possible

Abbreviations: ZER, zervamicin IIB; AMP, ampullosporin A; ANT, antiamoebin I; ALA, alamethicin; 5(16)-doxyl SA, 5(16)-doxyl stearic acid; PC, phospatidyl choline; DPoPC ($diC_{16:1}$ PC, 1,2-dipalmitoleoyl-*sn*-glycero-3-phosphocholine; POPC ($C_{16:0}/C_{18:1}$ PC), 1-palmitoyl-2-oleoyl-*sn*-glycero-3-phosphocholine; DOPC ($diC_{18:1}$ PC), 1,2-dioleoyl-*sn*-glycero-3-phosphocholine; DEiPC ($diC_{20:1}$ PC), 1,2-dieicosenoyl-*sn*-glycero-3-phosphocholine; LUV, large unilamellar vesicle; CD, circular dichroism; SA, surface associated; TM, transmembrane

* Corresponding author. Tel.: +31 715274419; fax: +31 715274537.
E-mail address: J.Raap@chem.leidenuniv.nl (J. Raap).

0005-2736/$ - see front matter © 2005 Elsevier B.V. All rights reserved.
doi:10.1016/j.bbamem.2005.07.001

mechanisms of their action are still under a discussion [4]. In the present study, membrane activities of the major representatives of intermediate length (15–16 residues), the peptaibols zervamicin IIB (ZER), antiamoebin I (ANT), ampullosporin A (AMP) were studied in a vesicular model system. The primary sequence of these neutral peptaibols is shown below (polar residues are underlined):

ZER: Ac-Trp[1]-Ile-Gln-Iva-Ile-Thr-Aib-Leu-Aib-Hyp-Gln-Aib-Hyp-Aib-Pro-Phl[16]
AMP: Ac-Trp[1]-Ala-Aib-Aib-Leu-Aib-Gln-Aib-Aib-Aib-Gln-Leu-Aib-Gln-Lol[15]
ANT: Ac-Phe[1]-Aib-Aib-Aib-Iva-Gly-Leu-Aib-Aib-Hyp-Gln-Iva-Hyp-Aib-Pro-Phl[16]

The primary structures of ZER and ANT are highly homologous at the C-terminal segment while the N-terminal segment of ANT is less polar. In contrast to ZER and ANT, AMP does not contain helix bending proline (Pro) or hydroxyproline (Hyp) residues. A common feature of ZER and AMP is the presence of a tryptophan (Trp) residue, which can act as an efficient membrane anchor. The molecular structures reported for the ZER analogues ([Leu[1]]-ZER [5]; ZER-IIB [6,7]) as well as for AMP [8] and ANT [9–11] are characterized by slightly bent helical conformations and a length long enough to span the apolar core of the lipid bilayer, which is a pre-requisite for channel formation. However, the regular distribution of polar/apolar residues, which is also essential for channel formation, appears to be more pronounced for ZER.

Previously, membrane activities were investigated for ZER, AMP and ANT in planar lipid bilayers [12–17]. Well-defined multilevel ion channels are formed by ZER in diphytanoyl PC membrane, which could be described by the barrel-stave model with $N=4–8$ helices per bundle [13]. The single channel conductance induced by ZER was shown to be comparable with that of ALA for similar experimental conditions [12]. Channel formation appears to be voltage-dependent with activation by a *cis*-positive membrane potential [3,13]. Substitution of the Trp[1] residue by Leu[1] in the ZER structure does not change the channel forming properties, while introduction of a negative charge ($Gln^3 \rightarrow Glu^3$) results in a *cis*-negative potential activation of this peptide [13].

The AMP-induced membrane macroscopic conductance in soybean PC membranes is a few orders of magnitude lower compared to ALA and other 19–20-residue peptaibols [16]. Native AMP isoforms (AMP-B, C, D) with Aib/Ala variations in the 8–10 segment are characterized by a comparable activity, while the Trp[1]-depleted analogue of AMP ([des-acetylTrp[1]]-AMP) is much less active under identical conditions [15,16]. Formation of single level channels was reported for ANT in POPC/DOPE but not for the diphytanoyl PC membrane. Compared to ALA, the process is less voltage-sensitive and requires higher concentrations of peptide [17]. The observed strong voltage-independent background conductance allowed the authors to suggest that the membrane activity of ANT might be also related to a carrier-like mechanism.

In spite membrane activities of ZER, AMP and ANT were previously characterized, a direct comparison of these peptaibols is hampered by the facts that different conditions (electrolyte, lipid, peptide concentration, etc.) were used and different experimental parameters were determined. Therefore, it was interesting to study the behaviour of these peptaibols under identical conditions and to reveal the factors determining their membrane activities. In contrast to previous studies, the vesicular membrane was selected as the model system of choice. Although studies of interactions of ANT and ZER with vesicles were reported [10,18–20], these data are not yet available for AMP. First, the affinities of peptaibols to PC membranes were studied by exploring the intrinsic fluorescence of the N-terminal Trp[1] residue (ZER and AMP) or by monitoring the circular dichroism (CD) spectra (ANT) in the presence of lipid vesicles. The thickness and lipid saturation level of the PC membranes were varied since both factors are known to be important for peptaibol incorporation. To localize the depth of peptaibol insertion into a PC bilayer, the Trp fluorescence quenching was monitored using water-soluble and membrane-bound quenchers. Finally, permeabilization of the PC vesicular membrane induced by peptaibols was studied by ion (K^+) leakage and membrane depolarization measurements. To clarify the role of the Trp[1] residue as well as that of the positive charge at the protonated terminal amino, it was of interest to compare the membrane permeabilization caused by the AcTrp[1]-depleted analogue of ZER with respect to the parent peptide. The activity of the peptaibols follows the order: ZER > AMP >> ANT > [des-acetylTrp[1]]-ZER which was shown to correlate with their binding affinities and the orientation/aggregation in the lipid bilayer.

2. Experimental

2.1. Materials

The following PC were purchased from Avanti Polar Lipids, Inc. or Sigma: DPoPC, DOPC, DEiPC, POPC, egg (chicken) PC. 5-Doxyl- and 16-doxyl stearic acids (5-doxyl(16)-SA) were obtained from Sigma. Ampullosporin A was prepared according to the literature [21]. Zervamicin-IIB was prepared as was described before [6].

2.2. Preparation of Trp- depleted zervamicin IIB

[Des-acetylTrp[1]]-ZER-IIB was obtained by chemical cleavage of ZER at the N-terminal residue with N-chlorosuccinimide (10 equivalents excess of the reagent, 27.5% acetic acid, 4 M urea) for 2 h at room temperature. The resulted mixture was separated by RP-HPLC on a Vydac column 208TP54 C8, 4.6×250 mm, 5 μm (Vydac,

USA). Purification of [des-acetylTrp^1]-ZER was achieved using the ternary mixture methanol/acetonitrile/water (67:14:19, v/v) at a flow rate 0.5 ml/min. The molecular mass of the isolated product was determined by TOF-MALDI mass spectrometry from the *m*/*z* 1632, which corresponds to the calculated mass of the sodium adduct $[M+Na]^+$of [des-acetylTrp^1]-ZER. The sample was shown to be pure by 600 MHz solution-state NMR spectroscopy.

2.3. Preparation of antiamoebin I

The fungus *Emericellopsis minima* (strain F1483), producing ANT, was obtained from the All-Russian Collection of Microorganisms (Moscow, Russia) and was grown in the fermentation medium containing 10 g of bacto peptone (Difco), 2.5 g of yeast extract (Difco), 10 g of starch, 10 g of glucose and 8 g of calcium carbonate per 1 L (pH 7.0). The culture was incubated for 6 days at 28 °C on a shaker at 220 rotations/min. Fermentation broth was filtered on a glass filter. The obtained filter cake was triturated with methanol (5 ml/g) and the methanol extract was dried in vacuum on a Speed Vac concentrator. The obtained solid was dissolved in a minimal volume of methanol and purified by RP-HPLC on a Symmetry Prep C18 column (7.8×300 mm, 7 μ, Waters, USA). Purification of ANT was achieved using a step gradient of the ternary mixtures methanol/acetonitrile/water A (60:5:35, v/v) and B (75:22.5:2.5, v/v). The gradient of 0–25% B was run for 5 min, of 25–40% B—for 30 min, and of 40–100% B—for 5 min at the flow rate 1.6 ml/min. The peptaibol was detected by A_{214}. The molecular mass of the isolated ANT was determined by TOF-MALDI mass spectrometry from the *m*/*z* 1693, which corresponds to the calculated mass of the sodium adduct $[M+Na]^+$ of ANT. The sample was shown to be pure by 600 MHz solution-state NMR spectroscopy.

2.4. Analysis of relative hydrophobicities

To compare the hydrophobicities of ZER, AMP, ANT and [des-acetylTrp^1]-ZER RP-HPLC retention times as well as capacity factors k′ were determined using a Symmetry Prep C18 column: 7.8×300 mm, 7 μ, Waters, USA. Isocratic elution (flow rate 1.6 ml/min) was performed using a 70 : 30 mixture of solvent A (60% methanol, 5% acetonitrile, 35% water) and solvent B (75% methanol, 22.5% acetonitrile, 2.5% water). The HPLC retentions times (min) and capacity factors (between brackets) determined for AMP, ZER, ANT and [des-acetylTrp^1]-ZER are 30.5 (5.35), 24.0 (4.00), 19.8 (3.13), 16.4 (2.73), respectively.

2.5. Binding experiments

A concentrated stock solution of ZER (AMP) was prepared by dissolving of a weighted sample in DMSO. This solution was used to prepare the “aqueous” solution of ZER(AMP) by its 100 fold dilution into a corresponding aqueous medium. PC LUV-100 vesicles were prepared by extrusion via a 0.1 μm polycarbonate filter in solution containing 200 mM Me_4NCl, 10 mM Tris–HCl (pH=7.4), 0.2 mM Na_2EDTA as described in [20]. The lipid concentration was determined by an enzymatic method using a commercially available kit (Boehringer Mannheim). Aliquots of a stock vesicular solution were added to a peptaibol solution in the same medium. All experiments were performed at room temperature (20±1 °C). Fluorescence emission spectra were measured in a 1-cm quartz cuvette with a Perkin-Elmer spectrofluorimeter (LS50B). The excitation wavelength was 280 nm and the excitation/emission slits were 2.5 mm. Spectra were base-line corrected by subtracting the background spectra of pure lipid vesicles for corresponding lipid concentrations.

For binding experiments in combination with CD measurements, the titrations were performed in the same way except that concentrated stock solutions of peptaibols were prepared in methanol. CD spectra were recorded with a Jobin-Yvon CD-6 spectrometer using a 1 cm path length cuvette. Spectra were collected over a range of 270–200 nm and subsequently base-line corrected and smoothed.

2.6. Fluorescence quenching experiments

Spin-labelled egg LUV-100 were prepared by evaporation of a chloroform/methanol solution of a mixture of PC and n-doxyl SA (n=5, 16), followed by hydration in the buffer (200 mM Me_4NCl, 10 mM Tris–HCl, 0.2 mM Na_2EDTA) and extrusion. The fraction of spin-labels in the membrane was varied by using different initial molar ratios of PC and n-doxyl SA. The membrane concentration of spin-label was determined by electron paramagnetic resonance spectroscopy (EPR) as follows. Vesicles were destroyed by addition of DMSO (to a final concentration of 75% (v/v)) and the intensity of resulting EPR spectrum was compared with the EPR spectra of standard solutions (0.1–0.4 mM 5(16)-doxyl SA in the same solvent system). All spectra were recorded at room temperature in a 1-mm diameter capillary tube with a JEOL (JES RE2X) spectrometer. The other experimental conditions were: microwave frequency ~9.5 GHz, modulation frequency 100 kHz, microwave power 1 mW, modulation amplitude 0.5 G, time constant 0.03 s and scan time 30 s.

Quenching of the Trp fluorescence by the membrane-bound 5(16)-doxyl SA was studied at room temperature by addition of spin-labelled vesicles to the aqueous peptide solution (C_P=0.7 μM) until peptide binding was completed. Quenching measurements using iodide were performed by addition of small aliquots of a 2 M NaI solution (containing 0.2 mM $Na_2S_2O_3$ to protect against I_2 formation) to the peptide (C_P=0.7 μM) that was completely bound to PC vesicles, i.e., for PC concentrations in the range of 10–80 μM (ZER) and 100–160 μM (AMP). All fluorescence spectra were base-line corrected and the signal intensities were measured at the fluorescence maxima.

2.7. Potassium influx measurements

Egg PC LUV-100, containing the entrapped fluorescent ion-selective indicator potassium benzofuran isophtalate (PBFI, Molecular probes, Inc.), were prepared in the medium containing 200 mM Me_4NCl, 10 mM Tris–HCl (pH=7.4), 0.2 mM Na_2EDTA and ~50 μM PBFI. The extravesicular indicator was removed by passing through a Sephadex G-50 column. The dissociation constant of the encapsulated PBFI complex with K^+ was determined as described in [20]. Under our experimental conditions the K_d value is 11.6 mM. For K^+ uptake studies the vesicles were diluted ~50 times into the medium containing 40 mM KCl, 160 mM Me_4NCl, 10 mM Tris–HCl (pH=7.4), 0.2 mM Na_2EDTA and subsequently the peptaibol solution in DMSO was added (final concentration of DMSO was less than 1%).

2.8. Membrane depolarization measurements

Aliquots of a stock solution of egg PC LUV-100 prepared in 200 mM KCl, 10 mM Tris–HCl (pH=7.4), 0.2 mM Na_2EDTA were diluted into solutions with variable concentrations of KCl and Me_4NCl (total concentration 200 mM) so that $[K^+]_{in} > [K^+]_{out}$. The diffusion potential $\Delta\psi = (RT/F)\ln([K^+]_{in}/[K^+]_{out})$, positive outside the vesicular membrane, was developed upon addition of valinomycin and was monitored with the potential-sensitive fluorescent probe safranine T (Riedel-de-Haen) [19]. The dissipation of $\Delta\psi$ was further observed by addition of a peptaibol solution to a suspension of polarized vesicles. All experiments were performed at room temperature.

2.9. Model calculations on peptaibol localization at polar–apolar interface

To mimic the interactions of a peptaibol with the hydrocarbon and polar regions of the lipid membrane, the model system with peptaibol molecule localized at the border of two solvents (octanol–water) was considered. The purpose was to find the optimal position of a peptaibol with respect to the interface between the solvents. This was achieved by calculation of the virtual "amphipathic plane", separating the molecule into hydrophobic and hydrophilic parts, which are buried in octanol and water, respectively. The most favoured orientation of this plane is determined by an optimal solvation of the amino acid side chains, based on their relative hydrophobicities and spatial positions (see below). For this purpose, a hydrophobicity scale was created for the proteinogenic and non-proteinogenic amino acid side chains, which is based on the $\log P_{octanol-water}$ values of a corresponding set of amino aldehydes. Partition coefficients of amino aldehydes were taken, instead of the more polar (zwitter ionic) amino acids, to better mimic the properties of the peptide residues. These values were determined by means of the molecular modelling program Spartan, operating under UNIX, using a module that allows calculating log*P* values of small molecules [22]. To test the validity of this approach, the empirically calculated log*P* values of Phe, Trp, Gln, Val, Ile, Leu and Thr were plotted versus the experimental $\log P_{octanol-water}$ values which were determined for the amino acid side chain derivatives, toluene, 3-methylindole, propionamide, propane, n-butane, isobutane and ethanol, respectively [23]. The plot showed a linear relationship, but the calculated log*P* values were systematically smaller compared to the experimental ones. For this reason, the log*P* values, used in the further calculation, were scaled to (log*P*)+1.4 and the following values were finally used: Phe (1.91), Phl (1.91), Ile (1.54), Leu (1.47), Lol (1.47), Trp (1.21), Val (1.13), Iva (1.12), Pro (0.74), Aib (0.63), Ala (0.24), Gly (−0.24), Hyp (−0,48), Thr (−0.30), Gln (−0.91).

The spatial position of the "amphipathic plane" with respect to the X-ray or NMR structure was found by selecting the plane (out of a large set of planes) for which $\sum[\log P(+)] - \sum[\log P(-)] = \log P(\text{total})$ was at maximum. (The first term of the equation is the sum of log*P* values of the atoms at the "hydrophobic" part of the molecule ($\sum[\log P] > 0$), while the second term is the same for the "hydrophilic" part ($\sum[\log P] < 0$)). Since the border between the two different phases, cannot be infinitely sharp the contribution of log*P* to the total sum was set zero at a thin space between the two phases. The width of this space was adjusted to the half of a C-C bond length (0.7 Å). The position of the "amphipathic plane" was calculated by a homemade program that was running on a Windows-PC using the MATLAB software package. Input data files contained co-ordinates of the amino acid side chain atoms (including the alpha carbon atoms) which were taken from the Protein Data Base (ZER, 1DLZ; ANT, 1GQO). The crystal structure of AMP [8] was kindly provided by M. Kronen (Hans-Knöll-Institut für Naturstoff-Forschhung, Jena, Germany) and J. Sühnel (Institut fur Anorganische und Analytische Chemie, Friedrich-Schiller-Universität, Jena, Germany). For the set of atomic positions of each i-th residue the hydrophobicity of the side chain atoms were defined by the quotient $(\log P^i)/N$, wherein $i = 1, 2, \ldots, N$ (including the C^α-atom). The spatial position of the optimal "amphipathic plane" in the co-ordinate system of the X-ray or NMR structure allowed to determine the shortest distance between any atom of the peptaibol to the octanol–water border, which coincided with the "amphipathic plane".

3. Results

3.1. Membrane binding of peptaibols

The environmental sensitivity of Trp fluorescence was used to study ZER and AMP interactions with PC membranes. POPC was chosen at first as a model synthetic

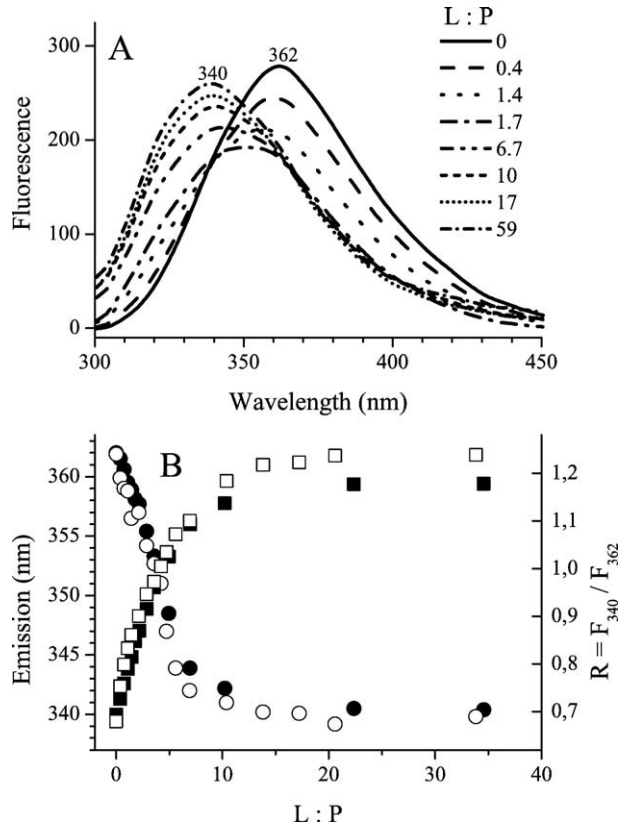

Fig. 1. (A) Fluorescence emission spectra of ZER in the presence of POPC at different lipid/peptide molar ratios. C_{ZER}=0.7 μM. (B) Position of the ZER fluorescence maximum (circles, left *Y*-axis) and ratio of fluorescence intensities at 340 and 362 nm (squares, right *Y*-axis) as a function of the lipid/peptide molar ratio. POPC (○, □), egg PC (●, ■); C_{ZER}=0.7 μM.

lipid representing the most abundant component of natural egg PC [24]. Fig. 1A illustrates that upon a stepwise addition of POPC vesicles to the ZER solution, a decrease of the fluorescence intensity as well as a gradual shift of the emission maximum from 362 nm to 350 nm is observed at low L/P ratios (<2.5) with an isosbestic point at 345 nm. Further increase of the POPC concentration shows another equilibrium (isosbestic point at 365 nm) characterized by the appearance of the fluorescence maximum at a wavelength of 340 nm. The equilibrium observed at low L/P ratios is characterized by a decrease of the fluorescence intensity, which suggests a strong aggregation of ZER upon binding to lipid. Formation of such ZER-enriched lipid aggregates can lead to the disruption of the bilayer structure. A membrane destabilization by ZER could be expected from recent solid state ^{31}P NMR experiments, which showed highly disordered headgroups of PC membranes at high peptide concentrations, whereas at low concentrations, no disturbance was found [25]. To confirm the possibility of membrane disruption, a Sephadex G-75 gel filtration column was loaded with a mixture of 1 mM PC and 0.5 mM ZER. After elution with the same electrolyte/buffer system as was used for binding studies, a very small amount of PC (~20%) was detected at the elution volume characteristic for ZER-free PC vesicles. Thus, at high P/L ratios ZER is capable to induce non-bilayer phases in PC system as was previously found for other peptides [26]. The fluorescence maximum at 340 nm observed at high L/P ratios likely corresponds to ZER associated with the non-disturbed vesicular membrane. To confirm this, a titration experiment was performed in the opposite direction, i.e., by adding increasing amounts of ZER (from 0.1 to 4 μM) to a vesicular solution with a high concentration of POPC (100–200 μM), so that the possibility of membrane disruption was minimized (data not shown). The final emission is observed at 340 nm, which thus indeed represents the fluorescence of a membrane-bound ZER. Fig. 1B shows that the limiting values of the emission maxima (λ_{max}) and ratios (R) of fluorescence intensities at 340 and 362 nm ($R=I_{340}/I_{362}$) upon lipid titration are achieved at L/P ≈ 15.

In Fig. 2A, the fluorescence emission spectra are shown for a titration of the AMP solution with POPC vesicles. The position of the fluorescence maximum of AMP in aqueous solution is the same as for ZER (362 nm), but the intensity of emission is smaller. On incorporation of AMP into PC membrane, a blue shift of the Trp fluorescence maximum is observed together with an overall increase of the fluorescence intensity. The maximum shift of fluorescence and the limiting R-value ($R=I_{346}/I_{362}$) are reached only at POPC

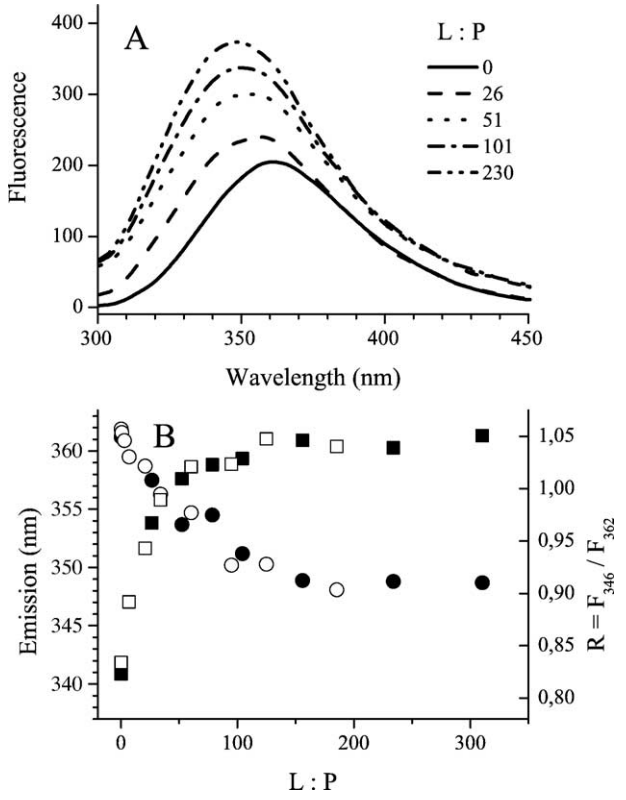

Fig. 2. (A) Fluorescence emission spectra of AMP in the presence of POPC at different lipid/peptide molar ratios. C_{AMP}=0.7 μM. (B) Position of the AMP fluorescence maximum (circles, left *Y*-axis) and ratio of fluorescence intensities at 346 and 362 nm (squares, right *Y*-axis) as a function of the lipid/peptide molar ratio. POPC (○, □), egg PC (●, ■); C_{AMP}=0.7 μM.

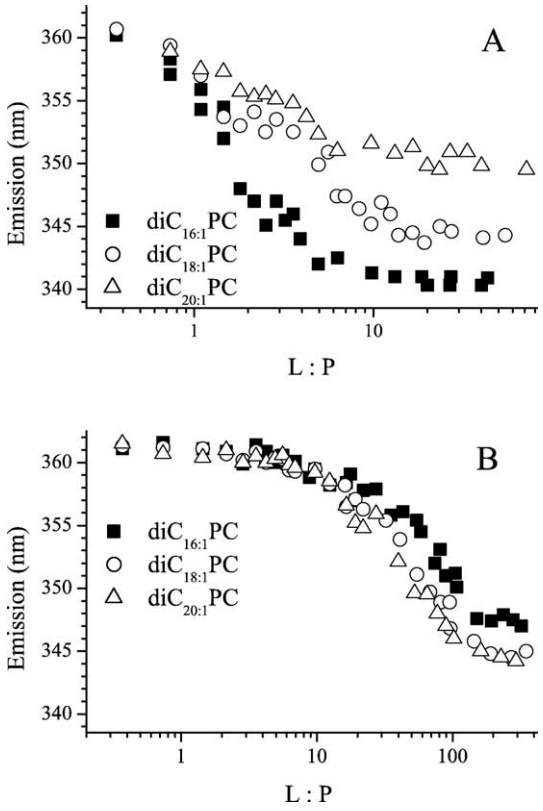

Fig. 3. Position of ZER (A) and AMP (B) fluorescence maxima as a function of the lipid/peptide molar ratio for different PC membranes. $C_{ZER}=C_{AMP}=0.7$ μM.

concentrations corresponding to L/P ≈ 150 (Fig. 2B), which suggests a ~10 times weaker membrane binding of AMP than ZER. Similar binding experiments performed with the natural egg PC, instead of POPC, show no changes in the position of fluorescence maxima and binding affinities for both ZER and AMP (Figs. 1B and 2B).

To see if the interaction of the peptaibol molecules with PC membrane can be influenced by the length of the lipid acyl chain and the related thickness of the bilayer, similar titration experiments were performed with vesicles prepared from different synthetic PC lipids ($diC_{16:1}PC$, $diC_{18:1}PC$, $diC_{20:1}PC$). The blue shift of the Trp emission observed upon addition to ZER (AMP) gave different limiting values of λ_{max} which depend on the type of lipid (Fig. 3 and Table 1). The position of the emission maximum is often used to determine the deepness of Trp insertion into the bilayer interior that determines the environmental polarity of the indole group [28]. A complication in the application of this method may arise when the Trp moiety is shielded from the lipid environment by neighbouring amino acid residues [29] or by peptide self-association [30]. However, the relatively short length of the peptide helix as well as the peripheral position of the (N-terminal) Trp residue of ZER (AMP) is expected to minimize these screening effects. Thus, the observed shift of λ_{max} upon ZER (AMP) binding to PC vesicles is due to changes of the local polarity of the Trp residue created by the membrane environment itself. The position of the fluorescence maximum at 350–340 nm suggests a location of Trp within the membrane interface with a slight penetration into the hydrophobic core [28]. This is in agreement with the preferable membrane interactions of the indole amino moiety with the carbonyl region of the bilayer and the fused aromatic rings with the lipid acyl chains [31,32].

For the membrane-incorporated ZER, a stronger blue shift is observed upon decreasing of bilayer thickness (Fig. 3A and Table 1). The dependency of the position of the indole side chain on the thickness of the hydrophobic core shows that the binding of this pepide is not restricted to the membrane surface. More reasonable is the explanation based on the assumption of a two-state equilibrium between the transmembrane (TM) and surface associated (SA) peptide in line with recent solid state NMR results of ZER [25]. For ZER as well as for a number of other peptides, it was demonstrated that the stability of the TM state of the peptide increases when the length of the hydrophobic peptide helix is matching the thickness of the hydrophobic core of the bilayer [28,30,33]. Indeed, the strongest blue shift of λ_{max} is observed for ZER (helix length 21–24 Å) in the $diC_{16:1}PC$ bilayer (thickness 23.5 Å) when the matching conditions are the most favourable. Thus, in this membrane, a higher TM fraction of ZER, characterized by a deeper inserted Trp, is present. The smaller blue shift observed for the ZER fluorescence in thicker PC bilayers suggests a more abundant SA peptide in response to an increased negative hydrophobic mismatch. In contrast to ZER, the position of Trp emission maximum observed for PC-bound AMP does not show a strong sensitivity to the bilayer thickness (Fig. 3B and Table 1).

Table 1
Characteristics of membrane-bound ZER and AMP

Lipid membrane	Hydrophobic bilayer thickness[a] (Å)	λ_{max} (ZER)[b] (nm)	λ_{max} (AMP)[b] (nm)	K (ZER)[c] (M^{-1})	K (AMP)[c] (M^{-1})
$diC_{16:1}PC$	23.5	340	347	$(2.0\pm0.2)*10^6$	$(5.0\pm0.1)*10^4$
$diC_{18:1}PC$	27.0	344	346	$(4.0\pm0.2)*10^5$	$(5.6\pm0.2)*10^4$
$diC_{20:1}PC$	30.5	350	345	$(3.1\pm0.1)*10^5$	$(5.8\pm0.1)*10^4$
$C_{16:0/18:1}PC$	26.0/27.0	340	348	$(8.5\pm0.3)*10^5$	$(5.7\pm0.1)*10^4$
Egg PC	~27	340	348	$(8.7\pm0.2)*10^5$	$(5.6\pm0.2)*10^4$

[a] Based on the distance between the two C^2 fatty acid carbons for $diC_{18:1}PC$ membrane [27], and 1.8 Å increment per one fatty acid carbon for the other monounsaturated lipids. For $C_{16:0}$ / $_{18:1}PC$ the length of corresponding acyl chains is given [27].
[b] Maximum of Trp emission.
[c] Apparent binding coefficient.

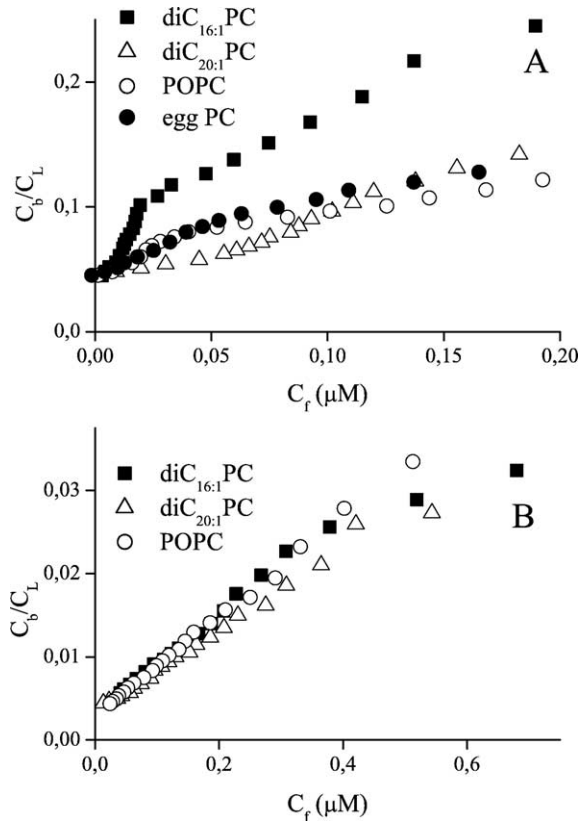

Fig. 4. Binding isotherms of ZER (A) and AMP (B) for different PC membranes.

Binding isotherms, i.e., plots of the amounts of bound peptide per lipid molecule (C_b/C_L) vs. concentrations of free (unbound) peptide (C_f), of ZER and AMP are shown in Fig. 4 for different PC membranes. The plots are based on the changes of R (the fluorescence intensity ratio) upon lipid addition (see Figs. 1B and 2B), assuming that the maximum limiting value of R corresponds to completely bound peptide. It should be noticed that in case of ZER the isotherms shown in Fig. 4A correspond to L/P ratios >3 and thus represent a binding of the peptide to the undisturbed vesicular membrane. In thin membranes, the initial region of the ZER isotherms is characterized by an upwards curvature (especially pronounced in case of the $diC_{16:1}PC$ membrane), which indicates that a peptide insertion/aggregation is involved in the binding process [34]. The apparent water–membrane partition coefficient ($K=C_b/(C_fC_L)$) was calculated by linear extrapolation of the initial slope of the C_b/C_L curve to $C_f\rightarrow 0$ (Table 1). The binding affinity of ZER is strongly influenced by the properties of the lipid acyl chains. ZER incorporation is favoured by decreasing of the membrane thickness, i.e. upon going from $diC_{20:1}$ to $diC_{16:1}$ PC bilayers. For membranes of similar thickness ($diC_{18:1}PC$ and $C_{16:0/18:1}PC$), a stronger interaction is observed with the more saturated lipid. In contrast to ZER, AMP binding curves are linear and almost insensitive to the properties of the membrane hydrophobic core. The affinity of AMP to all PC bilayers studied is also much weaker than that of ZER (Table 1).

To characterize the membrane binding of peptaibols lacking the fluorescent Trp residue (ANT and [des-acetylTrp^1]-ZER), the changes of their CD spectra in the presence of egg PC were studied. Parallel measurements with ZER were performed as a control (data not shown). The CD spectrum of the aqueous solution of ZER changes considerably upon addition of PC vesicles. The amplitude of the negative band at ~225 nm is strongly increased, suggesting an increase of peptide helicity. The titration curve of ZER shows its complete binding at ~15 μM PC (L/P ≈ 2), which is lower than found by fluorescence measurements due to the higher concentration of ZER used for CD studies. For ANT and [des-acetylTrp^1]-ZER at the same concentration the negative ellipticity is only slightly changed upon increasing of the PC concentration up to 100 μM (L/P ≈ 5) showing a very weak binding of these two peptaibols.

To further investigate the relationship between the depth of peptide insertion and acyl chain composition of the PC bilayers, the fluorescence quenching of the membrane-bound ZER and AMP was studied upon addition of water soluble iodide ions. In the absence of vesicles the Stern–Volmer plot ($F_0/F-1$ vs. $[I^-]$) is linear within the concentration range 0–180 mM of NaI giving similar values of the quenching constant (K_{SV}) for both peptides ($K_{SV}=13.9$ (±0.2) M^{-1} for ZER and $K_{SV}=13.3$ (±0.2) M^{-1} for AMP). On the other hand, for the membrane-bound peptides the Stern–Volmer plot showed negative deviations from linearity at NaI concentrations exceeding 50–70 mM. In this case, the modified Stern–Volmer relationship $F_0/(F_0-F)=1/f_a+1/(f_aK'_{SV}[I^-])$ was used to calculate the iodide-accessible fraction (f_a) and the effective quenching constant (K'_{SV}) [35]. The results of the calculations are shown in Table 2. The Trp residue of the membrane-bound peptides is only partially accessible to iodide and the K'_{SV} values are lower than those in the absence of vesicles. The accessibility factor and the K'_{SV} for ZER are higher in the thick bilayer ($diC_{20:1}$ PC) compared to the thin one ($diC_{16:1}$ PC), while the situation is reversed for AMP. Thus, ZER bound to thin membranes and AMP inserted into a thick bilayer have their Trp residues mostly shielded from the aqueous quencher, which is in agreement with the position of their emission maxima (Table 1). The iodide accessibility of both peptaibols bound to the egg PC membrane is reduced compared to membranes composed of synthetic mono-unsaturated lipids. Although iodide is thought to be a

Table 2
Fluorescence quenching by iodide of membrane-bound ZER and AMP

Lipid	f_a (ZER)	K'_{SV}(ZER), M^{-1}	f_a (AMP)	K'_{SV}(AMP), M^{-1}
$diC_{16:1}PC$	0.44 (±0.03)	5.0 (±0.2)	0.56 (±0.02)	7.6 (±0.1)
$diC_{20:1}PC$	0.51 (±0.03)	6.8 (±0.2)	0.58 (±0.05)	4.4 (±0.3)
Egg PC	0.30 (±0.03)	4.7 (±0.3)	0.36 (±0.05)	6.7 (±0.4)

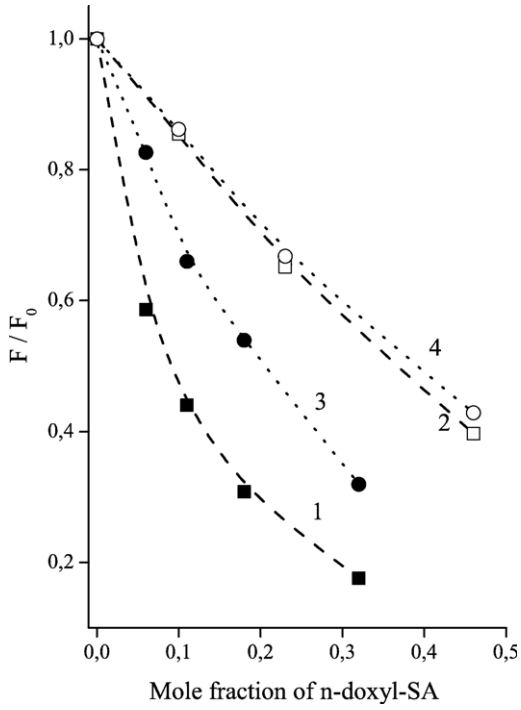

Fig. 5. Fluorescence quenching of ZER and AMP bound to egg PC vesicles containing different molar fraction of 5- and 16-doxyl SA. ZER-5-doxyl SA (1); ZER-16-doxyl SA (2); AMP-5-doxyl SA (3); AMP-16-doxyl SA (4). $C_{ZER}=C_{AMP}=0.7$ μM; $C_{PC}=80-160$ μM.

quencher for fluorophores located in the interface region, some penetration of iodide into the hydrophobic core also occurs [36]. Thus, the packing of lipid acyl chains can, to some extend, influence the quenching efficiency of iodide ions, which complicates the comparison between membranes composed of different PC. It is reasonable, that permeation of iodide into the hydrophobic region of the more rigid egg PC membrane is more restricted which explains the found lower f_a values.

To further examine peptide insertion into the egg PC membrane, the quenching of the Trp fluorescence by two membrane-incorporated spin-labelled stearic acids, 5- and 16-doxyl SA, was also studied. Since doxyl labels inserted into PC membrane are known to be able to quench within a distance of 11–12 Å [37], the 5-doxyl SA is expected to be an efficient quencher for Trp located at the membrane interface as well as in the hydrophobic core. In turn, 16-doxyl SA is only efficient for Trp inserted into the hydrophobic lipid interior. Fig. 5 shows that both 5- and 16-doxyl SA are able to quench the fluorescence of the membrane-bound peptides. In contrast to iodide quenching, when upon addition of iodide the emission maxima of Trp is slightly blue-shifted, the membrane-incorporated spin-labels shift the Trp emission to the longer wavelength region due to quenching of the more deeply located Trp. For both ZER and AMP, a stronger quenching is observed by a shallower located spin label due to the presence of peptides in the membrane interfacial region, which is inaccessible to the 16-doxyl SA quencher. The observed ~60% accessibility of Trp to the 16-doxyl SA quencher is in agreement with the finding that the remaining Trp is accessible to iodide (Table 2). Thus, the obtained results give a rough estimation of the ZER (AMP) fractions located into the hydrophobic core and at the interface of the egg PC membrane. A stronger quenching by 5-doxyl SA of ZER fluorescence than that of AMP indicates, on the average, a deeper membrane insertion of the former peptide, which is consistent with the positions of their fluorescence maxima observed in the egg PC membrane (Table 1).

3.2. Membrane activity of peptaibols

The ability of peptaibols to increase the membrane permeability was studied by measuring the K^+-flux through the egg PC bilayer. The K^+-transmembrane influx upon addition of the membrane-active peptide to the extravesicular KCl containing solution was followed by an increase of fluorescence of the vesicle-loaded potassium indicator PBFI [20]. At first, we proved that no leakage of PBFI from the intravesicular solution occurred upon addition of peptide to ensure that the increase of PBFI fluorescence is solely due to the transport of K^+ to the inside of the vesicles. To test this hypothesis, a concentrated (~6 mM) solution of PBFI-

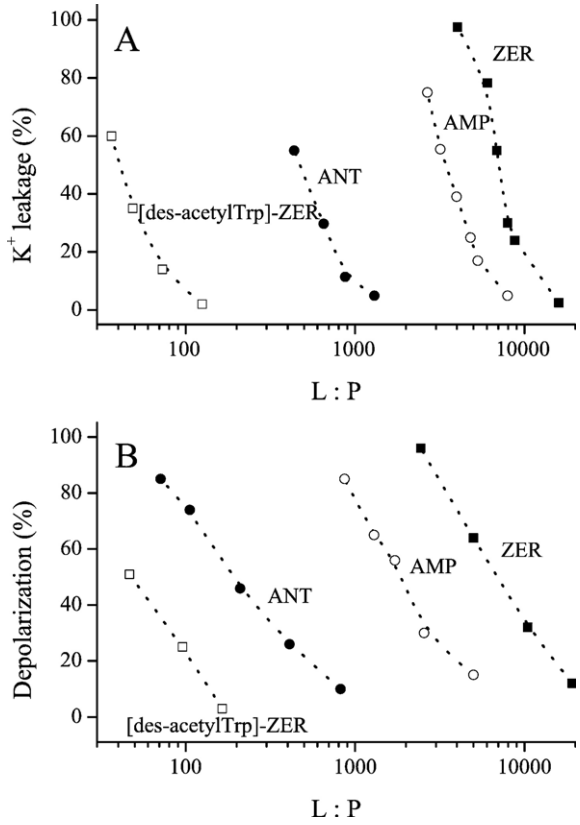

Fig. 6. (A) Peptaibol-induced K^+ leakage through the egg PC membrane and (B) peptaibol-induced dissipation of the transmembrane potential as a function of the lipid/peptide molar ratio. The percentages of leakage and depolarization (initial $\Delta\psi=+118$ mV) were determined 10 min after addition of the peptaibol to egg PC vesicles. $C_{PC}=350$ μM and 155 μM, respectively.

loaded vesicles was treated with 1–2 μM ZER (or other peptides) in the presence of extravesicular KCl for 30 min (incubation time and L/P ratios were similar to those used for further influx studies) during which PBFI fluorescence reached a stable level. Then, the vesicles were loaded on a Sephadex G-50 column and fractions were collected upon elution with an inert buffer. No free dye was present and all PBFI fluorescence was associated with the vesicle-containing fraction. Thus, under our conditions, no leakage of PBFI from the vesicular interior occurs and a detergent-like action of the peptaibols studied can be excluded under our conditions.

Next, the collected data were analyzed by conversion of the fluorescence intensities into the intravesicular K^+ concentration based on the preliminarily determined K^+-PBFI dissociation constant [20]. To quantify the membrane permeabilizing activity of different peptaibols, the intravesicular K^+ concentration obtained at 10 min after peptide addition (expressed in % with respect to its maximum value) was arbitrarily selected. Fig. 6A shows that an increase of peptide concentration (for a constant lipid concentration) results in an enhancement of K^+ leakage. The membrane activities of the peptaibols decrease in the order ZER > AMP >> ANT > [des-acetylTrp^1]-ZER and the respective L/P ratios required for half-maximal effect are given in Table 3.

The membrane activity of peptaibols was also studied in polarized egg PC vesicles where a *cis*-positive transmembrane potential $\Delta\psi = +118$ mV was installed by addition of the K^+-selective ionophore valinomycin. Dissipation of $\Delta\psi$ upon addition of all peptides, followed with potential sensitive dye safranine T, was observed, which is due to the outward flow of K^+ ions. The changes of safranine T fluorescence were recalculated into the drop of $\Delta\psi$ using a preliminary determined calibration curve as described in [19]. The relative order of depolarization activities (measured as the dissipated $\Delta\psi$ observed 10 min after addition of peptide) is the same as for the previously observed K^+ ion conduction (ZER > AMP >> ANT > [des-acetylTrp^1]-ZER) (Fig. 6B and Table 3). The latter two peptaibols are shown to be completely inactive in the concentration range L/P > 1000 wherein ZER and AMP are active. When comparing the activity curves obtained by the two methods, one could see that for all peptaibols (except [desTrp^1]-ZER) depolarization of vesicles takes place at lower L/P ratios than those required to cause K^+ influx. The increased activity in the polarized vesicles may reflect the activation of peptaibols by a *cis*-positive transmembrane potential as it was reported before for ZER in planar diphytanoyl PC bilayers [13] and egg PC vesicles [20].

Table 3
Membrane activity of peptaibols in egg PC vesicles

Peptaibol	L/P molar ratio displaying half-maximal effect on membrane permeabilization	
	K^+ uptake	Dissipation of $\Delta\Psi$
ZER	7000	5800
AMP	3500	1900
ANT	440	190
[des-acetylTrp^1]-ZER	44	48

4. Discussion

The peptaibols, ZER, AMP and ANT have been the subject of a number of studies for their ability to induce voltage-gated ion conductance by formation of channels in different model membranes [12–17]. Though it is generally believed that channels are formed through self-association of amphipathic helical molecules, the structural features required for this activity are not yet completely understood [4]. In the present study, the membrane activity of these three neutral peptaibols of similar length was investigated by measuring the flux of K^+ ions across the vesicular membrane and by studying the dissipation of the transmembrane potential. It was found that the membrane modifying activity decreases in the sequence: ZER > AMP >> ANT (Fig. 6 and Table 3). The activity of the channel forming peptaibol depends on the efficiency of the following steps: (a) partition of the peptaibol from water to the membrane surface, (b) transition from the surface-associated (SA) the transmembrane (TM) state and (c) aggregation of N-monomers into the ion-conducting bundle.

$$P_{aq} \Leftrightarrow P_{SA} \Leftrightarrow P_{TM} \Leftrightarrow P_{channel}$$

The apparent affinities of the peptaibols to the bilayer, probed by changes of Trp-fluorescence or by increase of negative ellipticity near 225 nm, were shown to decrease in the order ZER > AMP >> ANT > [des-acetylTrp^1]-ZER. Since hydrophobic interactions play a major role in the partitioning of peptides into the lipid bilayer [38,39], the relative hydrophobicities of the peptaibols were estimated from the reversed-phase HPLC retention times upon isocratic elution (AMP 30.5 min, ZER 24.0 min and ANT 19.8 min). The higher hydrophobicity of AMP than that of ZER could be inferred from the primary structures, but ANT was not expected to be more hydrophilic than ZER. Analysis of experimental 3D structures of the latter two peptaibols reveals that while the spatial structure of ZER in different environments (crystal state, solvents) appears to be almost identical [5–7], large differences were reported for crystal and solvent structures of ANT [10,11]. Thus, the secondary structure of ANT is not as rigid as that of ZER and the increased hydrophilicity of ANT might be due to more solvent exposed polar backbone peptide bonds at its flexible N-terminus.

The sequence of the membrane affinities (ZER > AMP >> ANT) does not completely follow the order of their hydrophobicities (AMP > ZER > ANT). The stronger membrane affinity of ZER, in spite its lower hydrophobicity, may

reflect an additional energetic contribution to the binding arising from TM insertion of peptide molecules with their concomitant self-association (see below) [34]. For the most hydrophobic AMP the possibility of peptide aggregation in water prior to membrane binding must also be taken into account. Indeed, the fluorescence intensity of AMP in water (but not in DMSO) is much lower than for ZER at equal concentrations (Fig. 1A and Fig. 2A) which might be due to self-quenching of the Trp fluorescence within AMP aggregates. Upon incorporation of AMP into PC membranes, the fluorescence was enhanced due to dissociation of aggregates like it was reported for other hydrophobic peptides [40,41]. Thus, the weaker membrane binding of AMP is partly the result of strong hydrophobic peptide–peptide interactions in aqueous solution. The poor binding of ANT may be also explained (in addition to its higher hydrophilicity) by the lack of a Trp residue in its structure which is known to act as an efficient membrane anchor [32]. The absence of Trp together with the increased hydrophilicity due to the protonated N-terminal amino-group explains the even more reduced membrane affinity of the des-acetylTrp-depleted ZER analogue. The same strong decrease of membrane association was found for [des-acetylTrp^1]-AMP [42], which in turn resulted in the failure of this compound to form ion channels in planar bilayers under conditions when AMP was active [16].

For a proper understanding of the peptaibols activity, it is also important, to consider their tendency to adopt the TM-oriented state with concomitant self-aggregation to bundles of peptide helices. Recent solid state ^{15}N-NMR data of ZER bound to *planar* oriented lipid membranes showed the transfer of in-plane to TM orientations upon going from thick (di$C_{18:1}$ PC) to thin (di$C_{12:0}$ PC and di$C_{10:0}$ PC) membranes [25]. It would thus be of interest to examine the possibility of such transition in *vesicular* membranes. The data of Table 1 show that the TM-oriented state of ZER in the membrane of moderate thickness (di$C_{16:1}$PC) is indeed more preferable compared to the thicker membranes. Thus, upon reducing of membrane thickness from 30.5 Å (di$C_{20:1}$PC) to 23.5 Å (di$C_{16:1}$ PC), the 10 nm blue shift observed for ZER is most likely due to a deeper insertion of Trp, associated with an increase of TM fraction. The adsorption isotherm determined for the di$C_{16:1}$ PC membrane shows a strong upward initial bending (Fig. 4A), which also indicates the existence of an insertion/self-assembling process upon binding [34]. The better hydrophobic matching upon decreasing of the bilayer thickness clearly increases the membrane affinity of ZER as is demonstrated by the binding coefficients (Table 1). The incorporation of ZER molecules into a membrane is sensitive not only to the thickness of the hydrophobic core, but depends also on the degree of unsaturation of the fatty acyl chains (Table 1). The stronger blue shift observed for $C_{16:0}$/$C_{18:1}$PC compared to di$C_{18:1}$PC (similar bilayer thickness) shows that the fraction of TM-associated ZER increases in the membrane composed of more saturated lipid (Table 1). This result is also in agreement with previous ^{15}N-NMR data where an equilibrium between the trans- and in-plane membrane orientation was found for ZER molecules in the $C_{16:0}$/$C_{18:1}$PC bilayer, while only the in-plane-orientated ZER was observed in the more unsaturated di$C_{18:1}$PC membrane [25]. Another consequence of increasing the saturation level of acyl chains is the stronger ZER binding (Table 1). A similar increase of the binding affinity to membranes composed of more saturated lipids was reported previously for ALA [43,44].

In contrast to ZER, the Trp fluorescence maximum as well as the binding affinity of AMP is not sensitive to the bilayer thickness and the level of lipid acyl chain unsaturation (Table 1). In the membrane of moderate thickness (di$C_{16:1}$ PC, egg PC) a more shallow localization of the Trp residue of AMP than that of ZER was demonstrated by quenching measurements with water soluble iodide ions (Table 2). A similar conclusion can be drawn considering the results of Trp quenching by 5- and 16-doxyl-SA incorporated into the egg PC membrane (Fig. 5). Compared to ZER, 5-doxyl SA causes a weaker quenching of AMP fluorescence, which indicates a less deep insertion of the latter peptaibol into the egg PC membrane. Thus, compared to ZER, a much smaller fraction of the membrane bound AMP is involved in formation of the TM state.

For AMP bound to the thick di$C_{20:1}$PC membrane, however, the blue shift of the fluorescence maximum is 5 nm more than that of ZER (Table 1) suggesting a more deeply buried Trp residue of AMP. The latter is also confirmed by a weaker iodide quenching observed for AMP (Table 2). In this membrane system, the SA state of both peptaibols becomes more energetically favourable because of the increased negative hydrophobic mismatch between peptide length and bilayer thickness [26]. To characterize the peptaibols binding parallel to the membrane surface, we performed model calculations on the localization of peptaibols at the membrane mimicking octanol–water interface as described in Experimental (Fig. 7). For ZER and ANT the results show that the shortest distance between the C7 carbon atom of the Trp side chain, buried in octanol, to the amphipathic plane is 5.5 Å and 10.5 Å, respectively, thus confirming the deeper Trp insertion for the latter peptide into a thick membrane as was found in our experiments. The method described above is attractive for a characterization of the localization of different peptides at the hydrophobic/hydrophilic interface based on their NMR and X-ray structures. Particularly, the information about the deepness of Trp (or any other residue) insertion cannot be obtained by other methods used to analyze the polarity of a peptide structure [45–47].

A pre-requisite of channel formation is the TM alignment of a helix which demands hydrophobic matching between membrane thickness and peptide length. The peptaibols studied here (15–16 residues) are long enough to make the TM orientation possible similar to 19/20-mer peptaibols such as the well-studied alamethicin. On the

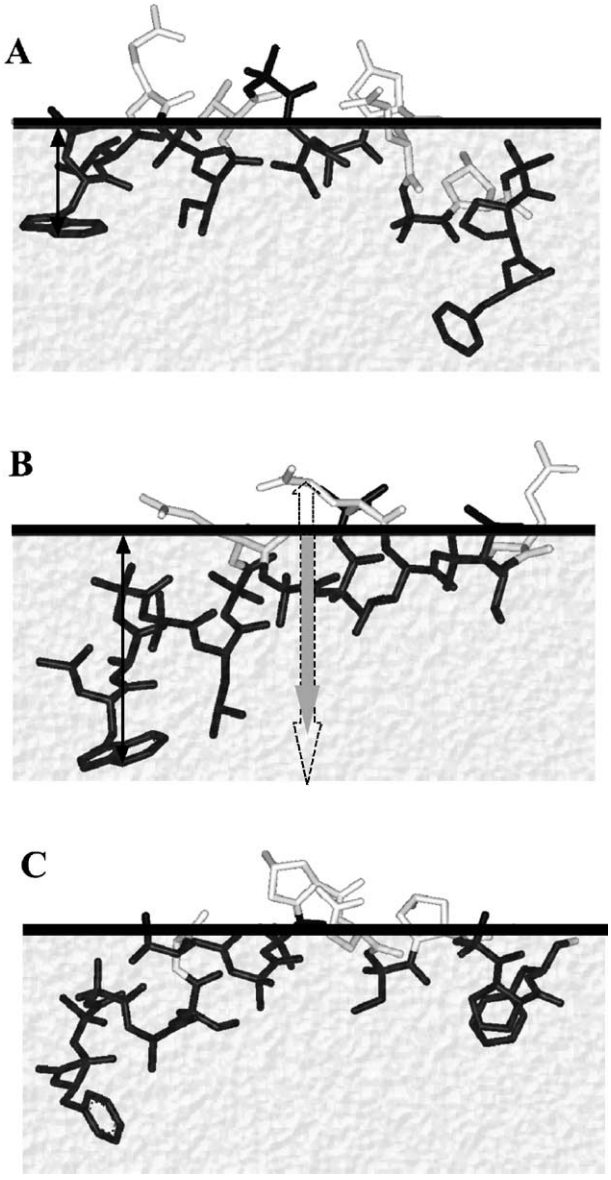

Fig. 7. Calculated orientations of ZER (A), AMP (B) and ANT (C) molecules at the octanol–water interface to mimic their membrane surface associated states. Peptide structures were taken from X-ray or NMR data (see Experimental). Hydrophobicities of the amino acid side chains were calculated on the bases of the suggested log *P* scale. Polar (log$P<0$) and apolar (log$P>0$) residues are shown here in white and black, respectively. The bold line shown indicates the perpendicularly oriented "amphipathic plane", separating the (overall) hydrophobic and hydrophilic faces of the helical molecule. The location of the indole group was calculated from the shortest distance between the coordinate of the C7-indole carbon atom and the "amphipathic plane" (ZER, 5.5 Å; AMP, 10.5 Å). The "amphipathic moment", defined by $\sum(\sum \log P(+)+\sum \log P(-))$, is shown for AMP and represented by a shaded vector. The individual $\sum \log P(+)$ and $\sum \log P(-)$ vectors are indicated by dotted arrows.

other hand, the TM state of amphipathic helices is stable only upon their subsequent self-association into an aggregate (channel, pore) to minimize the exposure of hydrophilic faces of the helices to the hydrophobic membrane interior. Stabilization of the peptaibol helix bundle involves hydrophobic interactions between the apolar face of peptide helix with lipid acyl chains and hydrogen bonding/ionic interactions between polar residues at the hydrophilic face as well [2,3,48,49]. From this point of view, the distribution of polar/apolar residues along the helical structure is another important factor for channel formation. As a measure of peptide amphipathicity, the hydrophobic moment calculated according to Eisenberg is widely used [46]. However, this method is restricted to only pure α-helical conformations of peptide sequences and could not be used for more complex helical structures, like for ZER with a mixed $\alpha/3_{10}$ conformation. To estimate the amphipathicity of a peptaibol, the experimentally determined 3D structure was divided into a hydrophobic and a hydrophilic sector, separated by a virtual plane (see Experimental). Then, the sum of log*P* values calculated for individual residues (see Experimental) located at each sector, determines the "hydrophobicity" and "hydrophilicity" of a peptide structure shown by the two opposing dotted vectors in Fig. 7. The sum of these vectors is considered to be a qualitative measure of the "amphipathic moment". The amphipathic moments for AMP, ZER and ANT (7.6, 8.8 and 10.2, respectively) demonstrate that the hydrophilic faces of all these peptaibols are dominated by the hydrophobic ones, which was shown before to be typical for ion-channel forming peptides [47]. It also appears that a rise of hydrophobicity is accompanied by a linear decrease of their amphipathicity. For instance, the relative large hydrophobicity of AMP is associated with a smaller amphipathicity. In this respect ZER is taking an intermediate position which makes it better candidate for channel formation. Indeed, empirical data for different proteins show that multimeric TM sequences are found in the central region of the Eisenberg's plot (hydrophobic moment vs. hydrophobicity), thus indicating the importance of the subtle balance between hydrophobicity and amphipathicity for the proper conditions of channel formation [50]. Compared to the regular distribution of polar residues along the hydrophilic face of the ZER helix, AMP and ANT show a smaller number of polar amino acids (3 vs. 5), which are clustered at the C-terminal end (Fig. 7). Molecular modelling studies of peptaibols channels revealed the importance of polar residues in stabilization of helix bundles [3,48,49]. This was also confirmed experimentally for ZER, ALA and harzianins HC analogues, which showed a decrease of channel activity upon replacement of hydrophilic residues by hydrophobic ones [13,51,52]. Thus, the less pronounced hydrophilic face of ANT helices is expected to diminish the efficiency of the $P_{TM} \Leftrightarrow P_{channel}$ step which relates well to the very weak activity of this peptaibol.

In conclusion, the performed study revealed that in spite of a similar length, the peptaibols studied have very different membrane-perturbing activities. The observed sequence of the decreasing membrane activity ZER-AMP-ANT can be explained by considering their binding affinities as well as by their orientation/aggregation states

in PC membranes. To reveal the role of different structural parameters in the permeabilization process, further systematic studies with natural peptaibols and their chemically modified analogues are required.

Acknowledgements

We are grateful to Dr. T.I. Kostromina and Mrs. N.V. Swischeva (Shemyakin-Ovchinnikov Institute of Bioorganic Chemistry, Moscow, Russia) for the experimental support. This work was granted by the Netherlands Organisation for Scientific Research (projects NWO No 047.015.015 and No. 047.014.017), the Russian Federal Target-Oriented Program "Integration of Science and High Education in Russia for the years 2002–2006" (project B 0095/1375) whose support is gratefully acknowledged.

References

[1] L. Whitmore, J.K. Chugh, C.F. Snook, B.A. Wallace, The peptaibol database: a sequence and structure resource, J. Pept. Sci. 9 (2003) 663–665.
[2] G.A. Wooley, B.A. Wallace, Model ion channels: gramicidin and alamethicin, J. Membr. Biol. 129 (1992) 109–136.
[3] M.S.P. Sansom, Alamethicin and related peptaibols-model ion channels, Eur. Biophys. J. 22 (1993) 105–124.
[4] J.K. Chugh, B.A. Wallace, Peptaibols: model for ion channels, Biochem. Soc. Trans. 29 (2001) 565–570.
[5] I.L. Karle, J.L. Flippen-Anderson, S. Agarwalla, P. Balaram, Crystal structure of [Leu^1]zervamicin, a membrane ion-channel peptide: implication for gating mechanism, Proc. Natl. Acad. Sci. U. S. A. 88 (1991) 5307–5311.
[6] T.A. Balashova, Z.O. Shenkarev, A.A. Tagaev, T.V. Ovchinnikova, J. Raap, A.S. Arseniev, NMR structure of the channel-former zervamicin IIB in isotropic solvents, FEBS Lett. 466 (2000) 333–336.
[7] Z.O. Shenkarev, T.A. Balashova, R.G. Efremov, Z.A. Yakimenko, T.V. Ovchinnikova, J. Raap, A.S. Arseniev, Spatial structure of zervamicin IIB bound to DPC micelles: implications for voltage-gating, Biophys. J. 82 (2002) 762–771.
[8] M. Kronen, H. Görls, H.-H. Nguyen, S. Reissmann, M. Bohl, J. Sühnel, U. Gräfe, Crystal structure and conformational analysis of ampullosporin A, J. Pept. Sci. 9 (2003) 729–744.
[9] I.L. Karle, M.A. Perozzo, V.K. Mishra, P. Balaram, Crystal structure of the channel-forming polypeptide antiamoebin in a membrane-mimetic environment, Proc. Natl. Acad. Sci. U. S. A. 95 (1998) 5501–5504.
[10] C.F. Snook, G.A. Wooley, G. Oliva, V. Pattabhi, S.P. Wood, T.L. Blundell, B.A. Wallace, The structure and function of antiamoebin I, a proline-rich membrane-active polypeptide, Structure 6 (1998) 783–792.
[11] T.P. Galbraith, R. Harris, P.C. Driscoll, B.A. Wallace, Solution NMR studies of antiamoebin, a membrane channel-forming polypeptide, Biophys. J. 84 (2003) 185–194.
[12] S. Agarwala, I.P. Mellor, M.S.P. Sansom, I.L. Karle, J.L. Flippen-Anderson, K. Uma, K. Krishna, M. Sukumar, P. Balaram, Zervamicin, a structurally characterised peptide model for membrane channels, Biochem. Biophys. Res. Commun. 186 (1992) 8–15.
[13] P. Balaram, K. Krishna, M. Sukumar, I.R. Mellor, M.S.P. Sansom, The properties of ion channels formed by zervamicins, Eur. Biophys. J. 21 (1992) 117–128.
[14] P.A. Grigoriev, A. Berg, R. Schlegel, U. Gräfe, Differences in ion permeability of an artificial bilayer membrane caused by ampullosporin and bergofungin, new 15-membered peptaibol-type antibiotics, Bioelectrochem. Bioenerg. 44 (1997) 155–158.
[15] P.A. Grigoriev, M. Kronen, B. Schlegel, A. Härtl, U. Gräfe, Differences in ion channel formation by ampullosporins B, C, D and semisynthetic desacetyltryptophanyl ampullosporin A, Bioelectrochemistry 57 (2002) 119–121.
[16] P.A. Grigoriev, B. Schlegel, M. Kronen, A. Berg, A. Härtl, U. Gräfe, Differences in membrane pore formation by peptaibols, J. Pept. Sci. 9 (2003) 763–768.
[17] H. Duclohier, C.F. Snook, B.A. Wallace, Antiamoebin can function as a carrier or as a pore-forming peptaibol, Biochim. Biophys. Acta 1415 (1998) 255–260.
[18] M.J. Das, K. Krishna, P. Balaram, Membrane modifying activity of four peptide components of antiamoebin, a microheterogeneous fungal antibiotic, Indian J. Biochem. Biophys. 25 (1988) 560–565.
[19] T.N. Kropacheva, J. Raap, Voltage-dependent interaction of the peptaibol antibiotic zervamicin II with phospholipid vesicles, FEBS Lett. 460 (1999) 500–504.
[20] T.N. Kropacheva, J. Raap, Ion transport across a phospholipid membrane mediated by the peptide trichogin GA IY, Biochim. Biophys. Acta 1567 (2002) 193–203.
[21] H.-H. Nguyen, D. Imhof, M. Kronen, B. Schlegel, A. Härtl, U. Gräfe, L. Gera, S. Reissmann, Synthesis and biological evaluation of analogues of the peptaibol ampullosporin A, J. Med. Chem. 45 (2002) 2781–2787.
[22] A.K. Ghose, A. Pritchett, G.M. Crippen, Atomic physicochemical parameters for three dimensional structure directed quantitative structure–activity relationships III: modelling hydrophobic interactions, J. Comput. Chem. 9 (1988) 80–90.
[23] A. Radzicka, R. Wolfenden, Comparing the polarities of the amino acids: side-chain distribution coefficients between the vapour phase, cyclohexane, 1-octanol and neutral aqueous solution, Biochemistry 27 (1988) 1664–1670.
[24] R.R.C. New (Ed.), Liposomes: A Practical Approach, Oxford Univ. Press, New York, 1990.
[25] B. Bechinger, D.A. Skladnev, A. Ogrel, X. Li, E.V. Rogozhkina, T.V. Ovchinnikova, J.D.J. O'Neil, J. Raap, ^{15}N and ^{31}P solid-state NMR investigations on the orientation of zervamicin II and alamethicin in phosphatidylcholine membranes, Biochemistry 40 (2001) 9428–9437.
[26] J.A. Killian, Hydrophobic mismatch between proteins and lipids in membranes, Biochim. Biophys. Acta 1376 (1998) 401–416.
[27] B.A. Lewis, D.M. Engelman, Lipid bilayer thickness varies linearly with acyl chain length in fluid phosphatidylcholine vesicles, Mol. Biol. 166 (1983) 211–217.
[28] J. Ren, S. Lew, Z. Wang, E. London, Transmembrane orientation of hydrophobic α-helices is regulated both by the relationship of helix length to bilayer thickness and by the cholesterol concentration, Biochemistry 36 (1997) 10213–10220.
[29] C.J. McKnight, M. Rafalski, L.M. Gierasch, Fluorescence analysis of tryptophan-containing variants of the LamB signal sequence upon insertion into a lipid bilayer, Biochemistry 30 (1991) 6241–6246.
[30] J. Ren, S. Lew, J. Wang, E. London, Control of the transmembrane orientation and interhelical interactions within membranes by hydrophobic helix length, Biochemistry 38 (1999) 5905–5912.
[31] W.-M. Yau, W.C. Wimley, K. Gawrisch, S.H. White, The preference of tryptophan for membrane interfaces, Biochemistry 37 (1998) 14713–14718.
[32] M.R.R. de Planque, J.A.W. Kruijtzer, R.M.J. Liskamp, D. Marsh, D.V. Greathouse, R.E. Koeppe II, B. de Kruijff, J.A. Killian, Different membrane anchoring positions of tryptophan and lysine in synthetic transmembrane α-helical peptides, J. Biol. Chem. 274 (1999) 20839–20846.
[33] U. Harzer, B. Bechinger, Alignment of lysine-anchored membrane peptides under conditions of hydrophobic mismatch: a CD, ^{15}N and ^{31}P solid-state NMR spectroscopy investigation, Biochemistry 39 (2000) 13106–13114.

[34] M.J. Zuckermann, T. Heimburg, Insertion and pore formation driven by adsorption of proteins onto lipid bilayer membrane–water interfaces, Biophys. J. 81 (2001) 2458–2472.
[35] S.S. Lehrer, Solute perturbation of protein fluorescence. The quenching of the tryptophyl fluorescence of model compounds and of lysozyme by iodide ion, Biochemistry 10 (1971) 3254–3263.
[36] M. Langner, S.W. Hui, Iodide penetration into lipid bilayers as a probe of membrane lipid organization, Chem. Phys. Lipids 60 (1991) 127–132.
[37] A. Chattopadhyay, E. London, Parallax method for direct measurement of membrane penetration depth utilizing fluorescence quenching by spin-labeled phospholipids, Biochemistry 26 (1987) 39–45.
[38] S.H. White, W.C. Wimley, Membrane protein folding and stability: physical principles, Annu. Rev. Biomol. Struct. 28 (1999) 319–365.
[39] M. Dathe, T. Wieprecht, Structural features of helical antimicrobial peptides: their potential to modulate activity of model membranes and biological cells, Biochim. Biophys. Acta 1462 (1999) 71–78.
[40] R.J. Webb, J.M. East, R.P. Sharma, A.G. Lee, Hydrophobic mismatch and the incorporation of peptides into lipid bilayers: a possible mechanism for retention in the Golgi, Biochemistry 37 (1998) 673–679.
[41] M.R.R. de Planque, E. Goormaghtigh, D.V. Greathouse, R.E. Koeppe II, J.A.W. Kruijtzer, R.M.J. Liskamp, B. de Kruijff, J.A. Killian, Sensitivity of single membrane-spanning α-helical peptides to hydrophobic mismatch with lipid bilayer: effect of backbone structure, orientation, and extent of membrane incorporation, Biochemistry 40 (2001) 5000–5010.
[42] H.-H. Nguyen, D. Imhof, M. Kronen, U. Gräfe, S. Reissmann, Circular dichroism studies of Ampullosporin A analogues, J. Pept. Sci. 9 (2003) 714–728.
[43] S. Stankowski, G. Schwarz, Lipid dependence of peptide–membrane interactions: bilayer affinity and aggregation of the peptide alamethicin, FEBS Lett. 250 (1989) 556–560.
[44] J.R. Lewis, D.S. Cafiso, Correlation between the free energy of a channel-forming voltage-gated peptide and the spontaneous curvature of bilayer lipids, Biochemistry 38 (1999) 5932–5938.
[45] M. Schiffer, A.B. Edmundson, Use of helical wheels to represent the structure of proteins and to identify segments with helical potential, Biophys. J. 7 (1967) 121–135.
[46] D. Eisenberg, R.M. Weiss, T.C. Terwilliger, The helical hydrophobic moment: a measure of the amphiphilicity of a helix, Nature 299 (1982) 371–374.
[47] R. Brasseur, Differentiation of lipid-associating helices by use of three-dimensional molecular hydrophobicity potential calculations, J. Biol. Chem. 266 (1991) 16120–16127.
[48] R.O. Fox, F.M. Richards, A voltage-gated ion channel model inferred from the crystal structure of alamethicin at 1.5 Å resolution, Nature 300 (1982) 325–330.
[49] M.S.P. Sansom, P. Balaram, I.L. Karle, Ion channel formation by zervamicin-IIB. A molecular modelling study, Eur. Biophys. J. 21 (1993) 369–383.
[50] D. Eisenberg, E. Schwarz, M. Komaromy, R. Wall, Analysis of membrane and surface protein sequences with the hydrophobic moment plot, J. Mol. Biol. 179 (1984) 125–142.
[51] M. Lucaciu, S. Rebuffat, C. Goulard, H. Duclohier, G. Molle, B. Bodo, Interaction of the 14-residue peptaibols, harzianins HC, with lipid bilayers: permeability modifications and conductance properties, Biochim. Biophys. Acta 1323 (1997) 85–96.
[52] L. Brachais, C. Mayer, D. Davoust, G. Molle, Influence of the secondary structure on the pore forming properties of synthetic alamethicin analogs: NMR and molecular modelling studies, J. Pept. Sci. 4 (1998) 344–354.